

A multiscale modeling of bone ultrastructure elastic proprieties using finite elements simulation and neural network method

Abdelwahed BARKAOUI^{1,2*}, Brahim TLILI^{1,2}, Ana VERCHER-MARTÍNEZ³, Ridha HAMBLI⁴

¹Université de Tunis El Manar, Ecole Nationale d'Ingénieurs de Tunis, LR-11-ES19 Laboratoire de Mécanique Appliquée et Ingénierie (LR-MAI), 1002, Tunis, Tunisie;

²Université de Tunis El Manar, Institut Préparatoire aux Etudes d'Ingénieurs d'El Manar, B.P 244, 2092, Tunis, Tunisie;

³Depto. de Ingeniería Mecánica y de Materiales, Centro de Investigación de Tecnología de Vehículos—CITV, Universitat Politècnica de València, Camino de Vera, 46022 Valencia, Spain

⁴PRISME laboratory, EA4229, University of Orleans Polytech' Orléans, 8, Rue Léonard de Vinci 45072 Orléans, France

Corresponding author:

Dr. Abdelwahed BARKAOUI

Université de Tunis El Manar

Ecole Nationale d'Ingénieurs de Tunis

LR-11-ES19 Laboratoire de Mécanique Appliquée et Ingénierie (LR-MAI)

1002, Tunis

Tunisia.

Phone: +216 27 660 279

Email: aabarkaoui@gmail.com

A multiscale modeling of bone ultrastructure elastic proprieties using finite elements simulation and neural network method

ABSTRACT

Bone is a living material with a complex hierarchical structure which entails exceptional mechanical properties, including high fracture toughness, specific stiffness and strength. Bone tissue is essentially composed by two phases distributed in approximately 30-70%: an organic phase (mainly type I collagen and cells) and an inorganic phase (hydroxyapatite-HA-and water). The nanostructure of bone can be represented throughout three scale levels where different repetitive structural units or building blocks are found: at the first level, collagen molecules are arranged in a pentameric structure where mineral crystals growth in specific sites. This primary bone structure constitutes the mineralized collagen microfibril. A structural organization of inter digitating microfibrils forms the mineralized collagen fibril which represents the second scale level. The third scale level corresponds to the mineralized collagen fiber which is composed by the binding of fibrils. The hierarchical nature of the bone tissue is largely responsible of their significant mechanical properties, consequently, this is a current outstanding research topic. Scarce works in literature correlates the elastic properties in the three scale levels at the bone nanoscale. The main goal of this work is to estimate the elastic properties of the bone tissue in a multiscale approach including a sensitivity analysis of the elastic behaviour at each length scale. This proposal is achieved by means of a novel hybrid multiscale modelling that involves neural network (NN) computations and finite elements method (FEM) analysis. The elastic properties are estimated using a neural network simulation that previously has been trained with the database results of the finite element models. In the results of this work, parametric analysis and averaged elastic constants for each

length scale are provided. Likewise, the influence of the elastic constants of the tissue constituents is also depicted. Results highlight that intelligent numerical methods are powerful and accurate procedures to deal with the complex multiscale problem in the bone tissue with results in agreement with values found in literature for specific scale levels.

Keywords: Bone ultrastructure, multiscale modelling, finite element method, neural network computation, elastics properties.

Introduction

Bone is a mineralized biological material which serves, among its other functions, as a structural support for other tissues in the body. The mechanical properties of bone have been naturally designed to fulfil this specific physiological function. In fact, in order to accomplish their biological and mechanical functions, bone hierarchical structure is constituted of many scale levels with specific interactions and a very complex architecture [1]. These structural scales can be distinguished as follows: macro-scale (whole bone), meso-scale (cortical and trabecular bone), micro-scale (single osteon and single trabecula), sub-micro-scale (lamella), nano-scale (microfibrils, fibrils and fibers), and sub-nanoscale (HA crystals and TC molecules) [2,3].

In order to analyse the equivalent mechanical behaviour of bone material, it is important to investigate the mechanical properties of its components and the structural relationships between them at different scales of hierarchical structural organization [4-6].

Many researchers in the literature have addressed this problem by developing analytical and numerical multiscale modelling of the bone mechanical behaviour [3,7-12]. These models use the homogenization and / or finite element technique to describe the mechanical behaviour of bone at certain scale levels. Some of these studies have focused on

Mineralized Collagen Microfibrils (MCMs) scale [13-17]. Others have been interested on the second scale level Mineralized Collagen Fibrils (MCFs) [18-21]. There are also works dealing with lamella scale [11,22] and osteons scale [12]. However, to the best of our knowledge, there are no studies focusing on the full multiscale description of bone hierarchical organization using numerical simulation methods.

Previous researchers have tried to approach bone multiscale organization by resorting to homogenization method. Some of them have estimated bone elastic properties. We can cite, as an example and not a limited list, the works of Martinez et al. [7] and Hamed et al. [3]. Others have evaluated fracture properties such as Fritsch and Hellmich [9] while Fritsch et al. [23] have extended their elastic multiscale micromechanical model for elasto-plastic analysis to predict cortical bone fracture toughness. Their findings mention that bone material fracture begins at the nano-scale at HA crystals and is followed by collagen cross-links fracture.

Concerning nano-structural scale levels, a particular attention has been given to the composition and structure of bone at these levels [24-27], the numerical modelling and experimental studies. There are few studies that focused on the MCMs scale level [3,13,15,16,28]. In the work of Barkaoui et al. [13] has been proposed a finite element geometrical model to study elastic mechanical properties and investigate the effect of some mechanical and geometrical parameters on the mechanical behaviour of mineralized collagen microfibril scale.

Scarce works are that referred to the Mineralized collagen Fibres (MCFRs) scale level. Yoon and Cowin [11] have studied mechanical properties of the tissue at the fibre scale by means of the homogenization method.

Most of works have been interested on mechanical behaviour and properties of individual MCF [29-32]. Several mechanical models have been developed in order to estimate the

mechanical properties of MCFs and bone tissues [9,33] and to model the 3D orthotropic elastic properties of a single MCF [34]. Nikolov and Raabe [10] proposed a homogenization method to model the elastic properties of bone at the mineralized MCF level from the staggered arrangement of collagen molecules up to an array of parallel MCF. Jaeger and Fratzl [35] proposed a model of MCF with a specific staggered arrangement of mineral particles distributed unequally in the gap and overlap zones of collagen fibrils. This geometric model has served as a reference for almost all the FEM models proposed for modelling bone at nano-scale. Jaeger and Fratzl [35] used this model to explore the effect of the mineral volume fraction and thickness as well as the distance of the HA platelets on the longitudinal elastic modulus, maximum elastic strain, and maximum elastic stress (strength) of the MCF. Kotha and Guzelsu [36] extended the Jaeger–Fratzl model [35] to investigate the effect of interphase and bonding on elastic properties of bone. Ji and Gao [37] used the same model geometry coupled with analytical formulation and a FEM analysis to obtain the transversely isotropic elastic constants of the MCF as a function of mineral aspect ratio. Yuan et al. [18] used a FEM analysis to predict the elastic properties of a MCF both in 2D and 3D and validated their computational results with experimental data obtained by synchrotron X-ray diffraction. They improved the shear lag Jaeger–Fratzl model [35] by incorporating more structural features of the MCF. To the best of our knowledge, this is the first MCF 3D model considering the staggered arrangement of HA crystal within the collagen matrix. Vercher-Martínez et al. [21] used a direct homogenization procedure by means of the finite element method and composite materials approaches to estimate the transversally isotropic properties of the MCF by considering the collagen and mineral distribution accordingly to the Hodge and Petruska model [38]. Molecular dynamics simulations (MD model) [39] have been developed to investigate the mechanical response under uniaxial tension of individual MCF. The results show that the deformation and failure mechanisms of a collagen fibril are strongly

influenced by its length and width as well as cross-linking density which, in turn, indicates the size dependence of failure mechanical properties of collagen fibrils.

In this study, we extend our previous models dealing with bone ultrastructure modelling in two aspects: (i) proposition of new 3D FE models to represent MCF and MCFR structures, (ii) development of a multiscale hybrid approach EF/NN of bone ultrastructure composed of three scale levels MCM, MCF and MCFR. This novel multiscale modelling is used to study the elastic properties of different bone tissue levels. Such model provides advantages when studying the effects of some parameters (geometrical or mechanical) related to the collagen, the mineral or the cross-links components on the strength of human bone.

2. Bone Ultrastructure

All researchers agreed on the fact that the bone in a nano-scope scale is essentially formed by two phases: organic phase is mainly composed of collagen type I representing [85-95%] [40] of the total protein in bone. The remaining bone organic matter consists of non-collagenous proteins (NCPs) and lipids. Inorganic phase is mainly composed of tiny crystals of apatite-like gold mineral hydroxyapatite (HA), $\text{Ca}_{10}(\text{PO}_4)_6(\text{OH})_2$ and water. The hierarchical combination of these components and the interconnection mechanisms between collagen molecules that provides stability and strength (cross-links), form a highly organized bone tissue. The length of the collagen molecule is approximately $4,4D$ [41] with $D=67$ nm being the periodic length between adjacent collagen molecules in the axial direction of the molecule. The period is composed by the gap or hole zone of $0,6D$ and the overlap zone of $0,4D$ [38]. The diameter of the collagen macromolecule is about 1.23 nm [42] and the lateral distance between adjacent molecules is 0.24 nm [43] in the absence of mineralization. This structure is repeated in the same way at different levels of scale forming a special building. This organization at the nano-scale is considered as multiscale structure. The transition

between different hierarchies of the ultrastructure scales is continuous rather than discrete in vivo bone. Although there is a general consensus on the classification of major scales, we accept some flexibility for intermediate levels. For example, Hamed et al. [8] reduce the number of scales by not considering the MCFR level between nano-scale (MCF) and the sub-microscopic level (lamella) in their study. On the other hand, Yang et al. [44] do not consider the existence of the MCMs. In contrast, in the present work, we consider that bone nano-architecture (ultrastructure) is formed by three basic structures which are: the mineralized collagen microfibrils (MCMs), the mineralized collagen fibrils (MCFs) and the mineralized collagen fibers (MCFRs) (see Fig. 1). MCFRs are formed by the assembly of MCFs surrounded by a matrix of mineral and are offset from each other with an apparent periodicity noted D . Then, MCFs are made the same way by MCMs related to each other by cross-links. Finally, MCMs, a particular assembly of five helical TC molecules, longitudinally offset them with the same apparent periodicity D .

[Insert Figure 1 about here]

In the following, we describe in more detail these three scale levels and their 3D FE modeling.

3. Method and tools

This section presents the hybrid multiscale modeling approach (Finite Element EF / Neural Network NN) of bone ultrastructure. This approach, which is summarized in Fig. 2, is composed of four steps: (i) development and simulation of geometric FE models for each level scale separately (microfibril, fibril and fiber), (ii) use of the results obtained from FE simulation in each scale level for the neural network program training phase,(iii)

generalization of the results in neural network prediction phase, (iv) transition between the different scales using the same NN program.

The forth step is constituted from three NN blocks assembled in series (NN block for each scale level) so each $NN(i+1)$ block uses as inputs the NNi block outputs (being $i=1,2$). Finally, $NN3$ outputs allow obtaining MCFR elastic properties.

[Insert Figure 2 about here]

Below, modeling with finite element methods and neural networks will be described in more detail. In section 3.1, we present the three proposed models of bone ultrastructure. A description of neural network method used for the generalization of the results and the multiscale transition is presented in Section 3.2.

3.1. Finite element model of scale levels

3.1.1. Mineralized Collagen Microfibril

From the work of Smith [46] several experimental works and observations highlight the presence of the microfibrils as the building block of the fibrils [47-52]. Basing on the previous references, Barkaoui et al. [13] have proposed a 3D modeling using finite elements method of the microfibril scale. By considering the work of Smith, the microfibril is defined as a hollow cylindrical pentameric arrangement of collagen molecules with an average diameter of 4 nm, generally known as Smith microfibril (see Fig. 3). Therefore, Barkaoui et al. [13] assume that microfibril is a helical assembly of five TC molecules (see Fig. 3), which are offset from each other with aperiodicity of 67 nm. This periodical length, D , is commonly used as a primary reference scale in describing the structural levels. Thereby, the helical length of a collagen molecule is approximately $4.34 D \approx 291$ nm and the discrete gap (hole zone) is $0.66 D \approx 44$ nm between two consecutive TC molecules in a strand. These gaps are the sites of nucleation for hydroxyapatite crystalline close packed structure.

[Insert Figure 3 about here]

3.1.2. Mineralized collagen Fibril/Fibre

In several researches, MCF is considered as a fiber reinforced composite characterized by short and stiff fibers (hydroxyapatite mineral platelets) embedded in a deformable matrix (cross-linked collagen molecules) at the collagen mineral scale [35]. Fig. 4 (a) represents an illustration of the real shape of mineralized collagen fibril which is composed of microfibril assembly formed in their turn by a specific cylindrical assembly of five TC molecules. Each one of these TC molecules is composed of three alpha helix chains.

Works using this model consider a periodic rectangular unit with definite geometric parameters [18,21,35,53]. In this work, the mineralized collagen fibril MCFs is considered as reinforced composite formed by a matrix of hydroxyapatite mineral platelets reinforced by deformable fibers (cross-linked mineralized collagen microfibrils) [54].

A new 3D finite elements geometric model of MCF is proposed in this study. Naturally, MCFs have a cylindrical shape with about 200 nm of diameter, but in this modeling a symmetrical and periodic square-shaped MCF portion having a length of about 10 nm is considered (see Fig. 4 (b)). The dimensions of the square is $< (1/20)$ of the MCF diameter, where the geometrical representation of a cylindrical shape by a square shape is mathematically acceptable (see Fig. 4). The microfibrils have cylinders form. These microfibrils are regularly distributed in the inorganic matrix (mineral) of the mineralized collagen fibril [54].

[Insert Figure 4 about here]

3.2. Neural network method description

From mathematical modeling side, we can define the NNs by the following four elements (i) The nature of the inputs and outputs, (ii) The total input function that defines pretreatment performed on the inputs, (iii) the neuron among activation function that defines its state based on its total input, (iv) output function that calculates NNs output depending on its activation state. NN is characterized by its ability to learn and generalize from experience and examples and to adapt to changing situations. After the training and testing phases, NNs is able to generalize rules and respond rapidly to inputs data in order to predict required outputs within the domain covered by the training example sand without a known relationship between data sets.

The NN model is a parallel processing architecture consisting of a large number of interconnected processing elements called neurons organized in layers. The single neuron performs a weighted sum of the inputs x_i that are generally the outputs of the neurons of the previous layer v_m , adding threshold value and producing an output given by:

$$v_m = \sum_{i=1}^L w_{im}x_i + b_i \quad (1)$$

Where w_{im} are the network weights.

Input signals cumulated in the neuron block are activated by a nonlinear function given by:

$$f(v_m) = 1/(1 + e^{(-\beta v_m)}) \quad (2)$$

The training process in the NN involves presenting a set of examples with known outputs. The system adjusts the weights of the internal connections to minimize errors between the network output and target output. There are several algorithms in a NN and the one used in the current analysis is the BP training algorithm. This algorithm is an iterative gradient procedure designed to compute the connection weights, minimizing the total mean square error between the actual output of the multilayer network and the desired output. In particular, the weights are initially chosen randomly and the rule consists on the comparison of the

known and desired output value with the calculating output value by using the current set of weights and threshold.

The mean square error is calculated by:

$$J = \left(\frac{1}{2P}\right) \sum_1^P \sum_{i=1}^N (D_{im} - \gamma_{im})^2 \quad (3)$$

Where γ_{im} is the actual output of the i th output node with regard to the m th training pattern, while D_{im} is the corresponding desired output. P and N denote respectively the total number of patterns and the number of output nodes.

The finite element modeling results of the bone ultrastructure scales, presented in the previous section were used for networks training.

To check its accuracy compared to FE method, the error is calculated according to the equation below comparing the two responses (FE and NN).

$$error = \frac{Var^{FE} - Var^{NN}}{Var^{FE}} \quad (4)$$

Where, Var represents the Young Modulus.

[Fig. 5](#) shows the NN prediction results compared with modeling results by EF. These results show good agreement between both technics (EF/NN) with a very low error value.

[Insert Figure 5 about here]

4. Results and Discussions

In this section, we present the most relevant results of the novel hybrid multiscale modeling performed in this work. [Fig. 6](#) shows the generalized results obtained by NN in the three scale levels MCM, MCF and MCFR. [Fig. 6](#) (a) represents the MCM equivalent Young's modulus as a function of the Young's modulus of the two essential bone constituents at this scale (mineral

and collagen). These results, obtained through NN1, are used in Fig. 6 (b) in order to represent the MCF equivalent Young's modulus as a function, at the same time, of the elastic properties of the mineral. In analogous way, the results of NN2 are used to determine the MCFR Young's modulus Fig. 6 (c). Note that the mineral is assumed to be at least in the matrix at every scale level. Our analyses bring the possibility of varying the Young's modulus of the mineral accordingly to the significant difference between amorphous and closely pack crystalline structure [18]. Fig. 6 shows that the mineral Young's modulus has a very significant effect compared to the effect of TC molecules Young modulus for the MCM level scale Fig. 6 (a) and a smaller effect compared with the effect of MCMs Young's modulus for the MCF scale level Fig 6 (b). These results are in good agreement with the results of finite element modeling [14,16]. By against, the curve of Fig. 6 (c) depicts that the MCFs Young's modulus has a greater effect on equivalent Young's modulus of MCFR compared to the mineral Young's modulus.

[Insert Figure 6 about here]

The elastic mechanical properties of bone ultrastructure scale levels depends on several geometrical and mechanical parameters such as Young's modulus bone elementary compounds (mineral, collagen) [16, 28], the nature of collagen (dry, wet) [15], size of the mineral crystal and the number of cross-links [28]. In order to clarify, the averaged elastic constants have been presented in table 1 to compare our results with experimental and numerical results of further works performed on the same components. There are few works focused on the mechanical properties characterization of MCFR, for this reason the comparison of the results is limited on MCM and MCF scale levels (see Figs. 7 and 8, respectively).

[Insert Table 1 about here]

Fig. 7 show a very good agreement between NN predicted (present work) and experimental results in the small strain regime based on X-ray diffraction [32], atomic force microscopy (AFM) [30] and molecular dynamics (MD) computation [17].

[Insert Figure 7 about here]

Fig. 8 also shows a good agreement between our NN predicted results for the MCF and numerical and experimental works: High-energy X-ray scattering [55], molecular dynamics (MD) computation [39] and finite elements method [18].

[Insert Figure 8 about here]

We note though a slight difference between the results of different studies. This can be explained by the different methods used, the size and nature (hydrated or dehydrated) of the MCM and MCF tested and the assumptions considered by each. In this study, for example, we neglect NCPs and consider mineral as a homogenized matrix without taking into account the presence of water. These assumptions can explain the differences mentioned above. However, seen living nature of the materials studied (bone), Young's modulus of MCM can be averaged about 1 ± 0.2 GPa and 40 ± 2 GPa for Young's modulus of MCF. Note again, that these elastic properties are highly dependent on several material and structural parameters of the scale studied. By varying one parameter, a large variation in elastic properties or also the properties at fracture can be produced. Finally, if initial conditions are specified we can give a unique value of the elastic properties of bone for every scale level. Make experimental tests or numerical simulations case by case can take much time and is expensive. Hence the growing interest in the use of intelligent numerical method, such as artificial neural networks method. This method provides great efficiency and precision. In this work, the combinations of artificial neuronal network method and finite element analysis have

been implemented and used to determine the mechanical elastic properties at different scale levels of the nanostructure of the bone tissue.

5. Conclusion

In this study, three 3D FE model for each nano-scopic structure of bone ultrastructure (MCM, MCF and MCFR) were proposed. Different numerical simulations were performed to identified the apparent behavior for each structure (global homogenized) and to identify the corresponding apparent mechanical properties. The proposed 3D geometric models were used to perform parametric studies to see the influence of geometrical and mechanical properties of the elementary constituents (HA crystals, TC molecules and cross-links) on the equivalent properties. In a second step, a multiscale approach using neural networks was developed. This approach uses the results of the finite element analysis for the training phase. It allows us to generalize the results obtained by finite element and do the transition between the different scale levels. The results were compared and validated by other studies from the literature and a good agreement was observed. This hybrid multiscale approach allows determining quickly (a few seconds) the mechanical equivalent properties as a function of the entered parameters. Here the method was only used to determine the elastic properties but can be approved to identify mechanical equivalent properties related to fracture behavior.

References

- [1] Sergey VD (2010). "Nanosized and nanocrystalline calcium orthophosphates." *Acta Biomaterialia* 6: 715–734.
- [2] Hamed E. and Jasiuk I. (2012) Elastic modeling of bone at nanostructural level, *Materials Science and Engineering R* 73 (2012) 27–49.
- [3] Barkaoui, A., Chamekh, A., Merzouki, T., Hambli, R. and Mkaddem, A., Multiscale approach including microfibril scale to assess elastic constants of cortical bone based on neural network computation and homogenization method. *Int. J. Numer. Meth. Biomed. Engng.* 30-3 (2014) 318-338
- [4] Mehta SS (1995). "Analysis of the mechanical properties of bone material using nondestructive ultrasound reflectometry." PhD Dissertation, The University of Texas Southwestern Medical Center at Dallas.
- [5] Landis WJ (1995). "The strength of a calcified tissue depends in part on the molecular structure and organization of its constituent mineral crystals in their organic matrix." *Bone* 16:533–44.
- [6] Weiner S, Traub W (1992). "Bone structure: from angstroms to microns." *FASEB* 6:879–85.
- [7] Martínez-Reina J, Domínguez J, García-Aznar JM. Effect of porosity and mineral content on the elastic constants of cortical bone: a multiscale approach. *Biomech Model Mechanobiol* 2011; 10:309–322.
- [8] Hamed E, Lee Y, Jasiuk I. Multiscale modeling of elastic properties of cortical bone. *Acta Mechanica* 2010; 213:131–154.
- [9] Fritsch A, Hellmich C. Universal microstructural patterns in cortical and trabecular, extracellular and extravascular bone materials: micromechanics-based prediction of anisotropic elasticity, *J. Theor. Biol.* 244(2007)597–620.
- [10] Nikolov S, Raabe D. Hierarchical Modeling of the Elastic Properties of Bone at Submicron Scales: The Role of Extrafibrillar Mineralization. *Biophysical Journal* (94) (2008) 4220–4232.
- [11] Yoon YJ, Cowin SC. The estimated elastic constants for a single bone osteonal lamella. *Biomechanics and Modeling in Mechanobiology* (2008a) 7:1–11.
- [12] Yoon YJ, Cowin SC. An estimate of anisotropic poroelastic constants of an osteon. *Biomechanics and Modeling in Mechanobiology* (2008b); 7:13–26.

- [13] Barkaoui A, Bettamer A, Hambli R. Failure of mineralized collagen microfibrils using finite element simulation coupled to mechanical quasi-brittle damage, *Procedia Engineering* 10 (2011) 3185–3190.
- [14] Barkaoui A, Hambli R. Finite element 3D modeling of Mechanical Behaviour of Mineralized collagen Microfibril, *J Appl Biomater Biomech* 9-3 (2011) 207 – 213.
- [15] Hambli R, Barkaoui A. Physically based 3D finite element model of a single mineralized collagen microfibril, *Journal of Theoretical Biology* 301(2012)28–41.
- [16] Barkaoui A, Hambli R. Nanomechanical properties of mineralised collagen microfibrils based on finite elements method: biomechanical role of cross-links. *Computer Methods in Biomechanics and Biomedical Engineering*, 17-14(2014)1590-1601.
- [17] Gautieri A, Vesentini S, Redaelli A, Buehler MJ. Hierarchical structure and nanomechanics of collagen microfibrils from the atomistic scale up. *Nano Letters*, 9-11(2)(2011)757–766.
- [18] Yuan F, Stuart R. Stock, Dean R. Haeffner, Jonathan D. Almer, David C. Dunand, L. Catherine Brinson. A new model to simulate the elastic properties of mineralized collagen fibril, *Biomech Model Mechanobiol* 10(2011)147–160.
- [19] Ghanbari J, Naghdabadi R. Nonlinear hierarchical multiscale modeling of cortical bone considering its nanoscale microstructure. *Journal of Biomechanical Engineering* 2009; 42:1560–1565.
- [20] Sansalone V, Thibault L, Salah N. Variational homogenization for modeling fibrillar structures in bone. *Mechanics Research Communications* 2009; 36:265–273.
- [21] Vercher-Martínez, A. , Giner, E., Arango, C., Javier Fuenmayor, F. Influence of the mineral staggering on the elastic properties of the mineralized collagen fibril in lamellar bone, *Journal of the Mechanical Behavior of Biomedical Materials*, 42(2015) 243-256.
- [22] Vercher A, Giner E, Arango C, Tarancón JE, Fuenmayor FJ. Homogenized stiffness matrices for mineralized collagen fibrils and lamellar bone using unit cell finite element models. *Biomech Model Mechanobiol* 13(2014) 437-449.
- [23] Fritsch A, Hellmich C, Dormieux L. Ductile sliding between mineral crystals followed by rupture of collagen crosslinks: experimentally supported micromechanical explanation of bone strength. *Journal of Theoretical Biology* 2009; 260(2):230–252.
- [24] M.J. Olszta, X.G. Cheng, S.S. Jee, R. Kumar, Y.Y. Kim, M.J. Kaufman, E.P. Douglas, L.B. Gower, *Bone Structure and Formation: A New Perspective Materials Science & Engineering R-Reports* 58(2007), 77–116.

- [25] N. Sasaki, A. Tagami, T. Goto, M. Taniguchi, M. Nakata, K. Hikichi, Atomic force microscopic studies on the structure of bovine femoral cortical bone at the collagen fibril-mineral level. *Journal of Materials Science-Materials in Medicine* 13(2002), 333–337.
- [26] E. Seeman, P.D. Delmas. The material and structural basis of bone strength and fragility *The New England Journal of Medicine* 356(2006), 2250–2261.
- [27] F.-Z. Cui, Y. Li, J. Ge, Self-assembly of mineralized collagen composites *Materials Science and Engineering R* 57(2007), 1–27.
- [28] Barkaoui, A., Hambli, R., Tavares, J.M.R.S. Effect of material and structural factors on fracture behaviour of mineralised collagen microfibril using finite element simulation, *Computer Methods in Biomechanics and Biomedical Engineering* 18-11(2015)1181-1190
- [29] Fei Hang and Asa H. Barber Nano-mechanical properties of individual mineralized collagen fibrils from bone tissue. *R. Soc. Interface.* 8(2011)500–505.
- [30] Van der Rijt JAJ, van der Werf KO, Bennink ML, Dijkstra PJ, Feijen J. Micromechanical testing of individual collagen fibrils. *Macromolecular Bioscience*, 6(9) (2006), 697-702.
- [31] Eppell SJ, Smith BN, Kahn H, Ballarini R, Nano measurements with micro-devices: mechanical properties of hydrated collagen fibrils. *Journal Of The Royal Society Interface*, 3(6) (2006), 117-121.
- [32] Shen ZL, Dodge MR, Kahn H, Ballarini R, Eppell SJ (2008) Stress-strain experiments on individual collagen fibrils. *Biophysical Journal*, 95(8) (2008), 3956-3963.
- [33] Akkus O. Elastic deformation of mineralized collagen fibrils: an equivalent inclusion based composite model. *Trans. ASME.*127(2005)383– 390.
- [34] Akiva U, Wagner HD, Weiner S. Modeling the threedimensional elastic constants of parallel-fibered and lamellar bone. *J. Mater. Sci.* 33(1998)1497–1509.
- [35] Jäger I, Fratzl P. Mineralized collagen fibrils: a mechanical model with a staggered arrangement of mineral particles. *Biophys. J.* 79 (2000)1737–1746.
- [36] Kotha S.P., Guzelsu N. The effects of interphase and bonding on the elastic modulus of bone: changes with age-related osteoporosis. *Medical Engineering & Physics* 22(2000), 575–585.
- [37] Ji, B. H., Gao H. J. Elastic properties of nanocomposite structure of bone. *Compos. Sci. Technol.* 66(2006), 1212-1218.

- [38] A.J. Hodge, J.A. Petruska, in: G.N. Ramachandran (Ed.), *Recent Studies with the Electron Microscope on Ordered Aggregates of the Tropocollagen Molecule*, Academic Press, New York, 1963, p. 289.
- [39] Buehler MJ. Nanomechanics of collagen fibrils under varying cross-link densities: atomistic and continuum studies. *Journal of the Mechanical Behaviour of Biomedical Materials* 1 (1) (2008), 59–67.
- [40] Shashindra MP, Katti KS, Katti DR. Multiscale model of collagen fibril in bone: elastic response. *J. Eng. Mech.* 140(2014) 454-461.
- [41] Boedtker .H and Doty. The Native and Denatured States of Soluble Collagen. *J. Am. Chem. Soc.* 78:4267-4280.
- [42] Landis W.J., Song M.J., Leith A., McEwen L., McEwen B. Mineral and organic matrix interaction in normally calcifying tendon visualized in three dimensions by high voltage electron microscopic tomography and graphic image reconstruction. *J Struct Biol.* 1993;110:39–54
- [43] Lees.S, Considerations regarding the structure of the mammalian mineralized osteoid from viewpoint of the generalized packing model. *Connective Tissue Research* 16 (1987) 281 – 303.
- [44] Yang L, Van der Werf KO, Dijkstra PJ, Feijen J, Bennink ML. 2012. Micromechanical analysis of native and cross-linked collagen type I fibrils supports the existence of microfibrils. *J Mech Behav Biomed Mater.* 6:148–158.
- [45] Angelo K, Christopher R, et al (2012). “Significant deterioration in nanomechanical quality occurs through incomplete extrafibrillar mineralization in rachitic bone: evidence from in-situ synchrotron X-ray scattering and backscattered electron image.” *Jouranal of bone and minral research*27 (4): 876-890.
- [46] Smith JW. 1968. Molecular pattern in native collagen. *Nature.* 219:157–158.
- [47] Raspanti M, Congiu T, Guizzardi S (2001). “Tapping-mode atomic force microscopy in fluid of hydrated extracellular matrix.” *Matrix Biol*20: 601-604.
- [48] Habelitz S, Balooch M, Marshall SJ, Balooch G, Marshall GW (2002). “In situ force microscopy of partially demineralized human dentin collagen fibrils.” *J. Struct. Biol*138: 227-236.
- [49] Baselt DR, Revel JP, Baldschwieler JD (1993). “Subfibrillar structure of type I collagen observed by atomic force microscopy.” *Biophys. J.*65:2644-2655.

- [50] Holmes DF, Gilpin CJ, Baldock C, Ziese U, Koster AJ, Kadler KE, Corneal collagen fibril structure in three dimensions: structural insights into fibril assembly, mechanical properties, and tissue organization. *Proc. Natl. Acad. Sci. USA*98 (2001), 7307-7312.
- [51] Orgel JPRO, Miller A, Irving TC, Fischetti RF, Hammersley AP, Wess TJ. The in situ supermolecular structure of type I collagen, *Structure* 9(2001) 1061-1069.
- [52] Orgel. JPRO, IrvingTC, MillerA. Wess TJ, Microfibrillar structure of type I collagen in situ, *Proceedings of the National Academy of Sciences of the United States of America*103: (2006),9001–9005.
- [53] Khaterchi, H. , Chamekh, A., BelHadjSalah, H. Artificial Neural Network analysis for modeling fibril structure in bone, *International Journal of Precision Engineering and Manufacturing* 16-3, (2015)581-587.
- [54] Barkaoui, A., BETTAMER, A., HAMBLI, R., Mechanical behaviour of single mineralized collagen fibril using finite element simulation coupled to quasi-brittle damage law, *ECCOMAS 2012, September 10-14, e-Book Full Papers (2012)*, PP 1357-1365.
- [55] Almer JD, Stock SR. Micromechanical response of mineral and collagen phases in bone. *J StructBiol* 157(2007), 365–370.

TABLE CAPTIONS

Table1- The average elastic mechanical properties of the bone ultrastructure scales.

FIGURE CAPTIONS

Fig. 1- Ultrastructure of the bone: (a) Full SEM MCFs [45], (b) collagen fiber, collagen fibril and microfibril with mature mineral in gap collagen zones (c) collagen fiber, fibril collagen and collagen microfibril with mature mineral gap in areas covered by the immature amorphous mineral.

Fig. 2- Hybrid (FE/NN) multiscale modeling of bone ultrastructure.

Fig. 3- Mineralized collagen microfibril structure.

Fig. 4- New 3D finite element model of MCF (a) grouping of MCMs in MCF, (b) 3D finite element model of portion MCF.

Fig. 5 - Comparison between finite element and neural network prediction results.

Fig. 6- Evolution of elastic moduli (GPa) of MCM and MCF as function of the mineral Young's modulus and passage between the MCM and MCF.

Fig. 7- Comparison between NN predicted Average Young's modulus of MCM and literature results.

Fig. 8- Comparison between NN predicted Average Young's modulus of MCF and literature results.

FIGURES

Figure 1

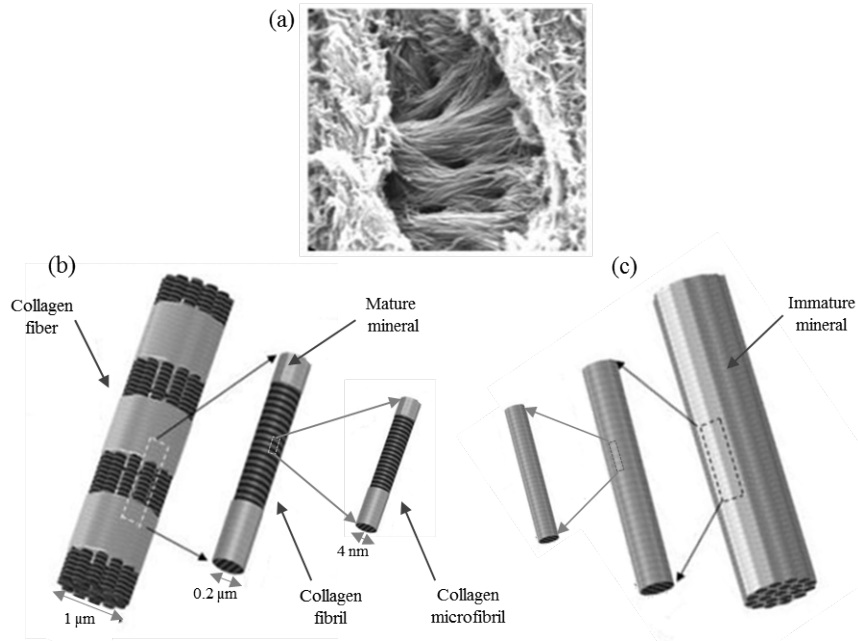


Figure 2

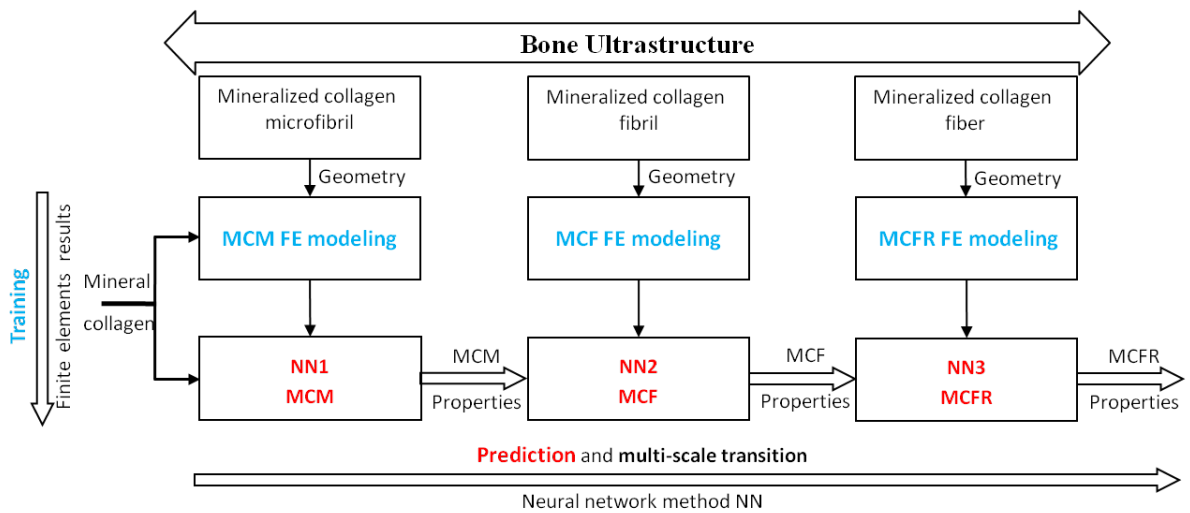


Figure 3

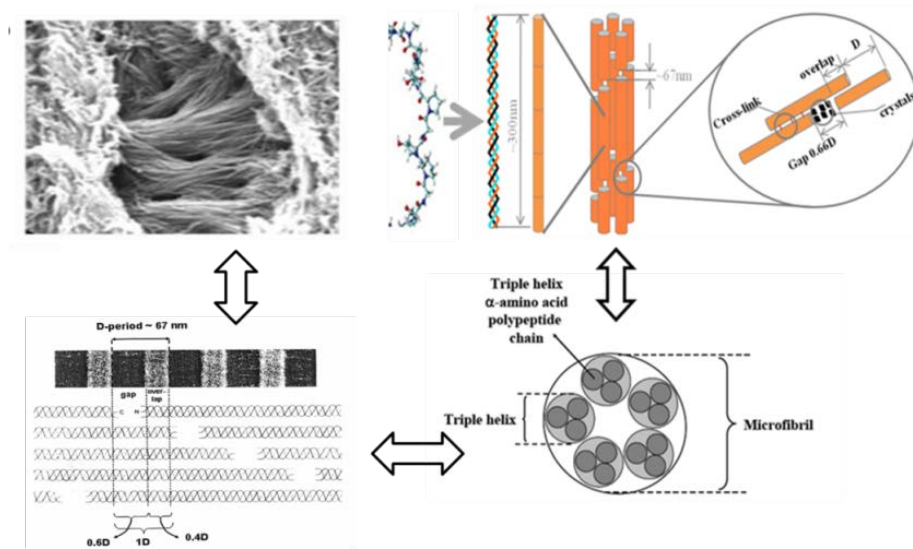


Figure 4

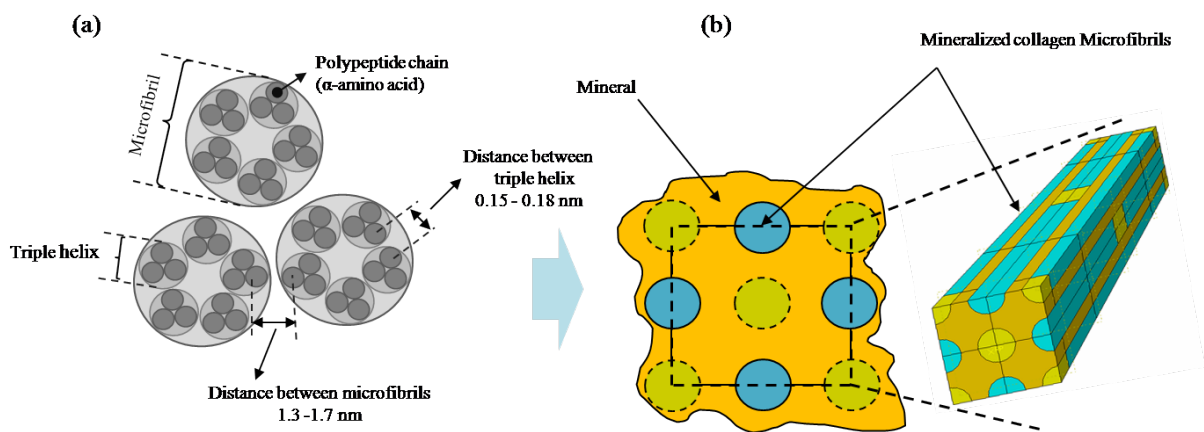
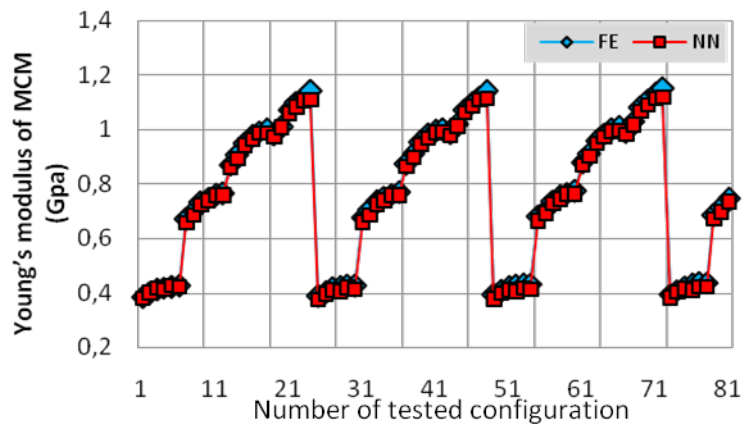
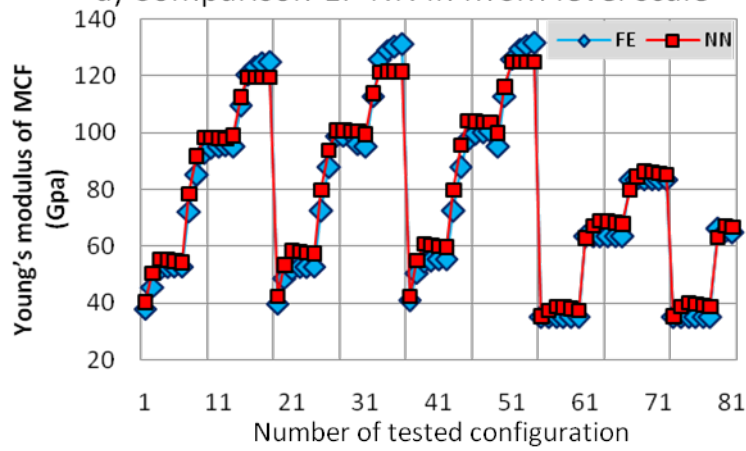


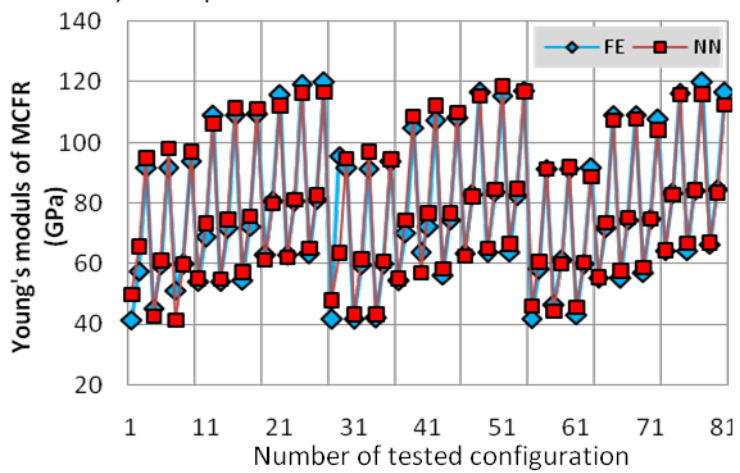
Figure 5



a) Comparison EF-NN in MCM level scale



b) Comparison EF-NN in MCF level scale



c) Comparison EF-NN in MCFR level scale

Figure 6

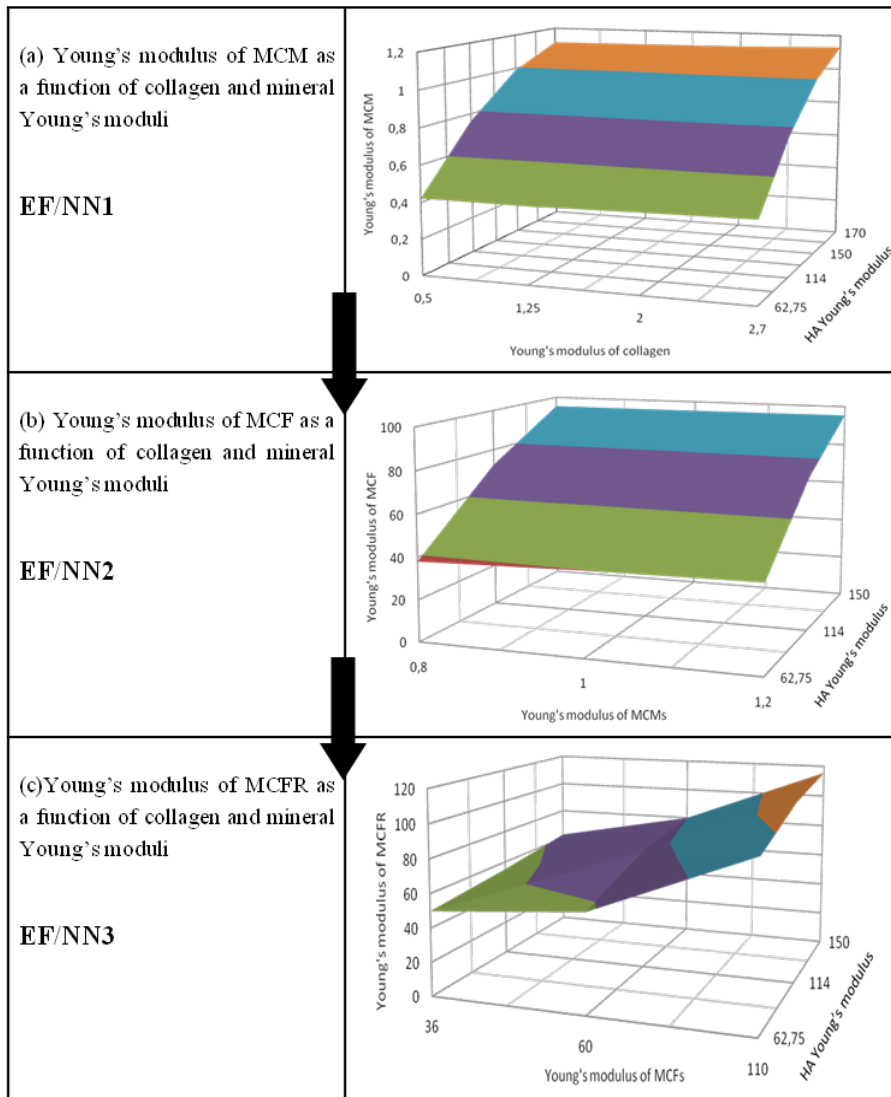


Figure 7

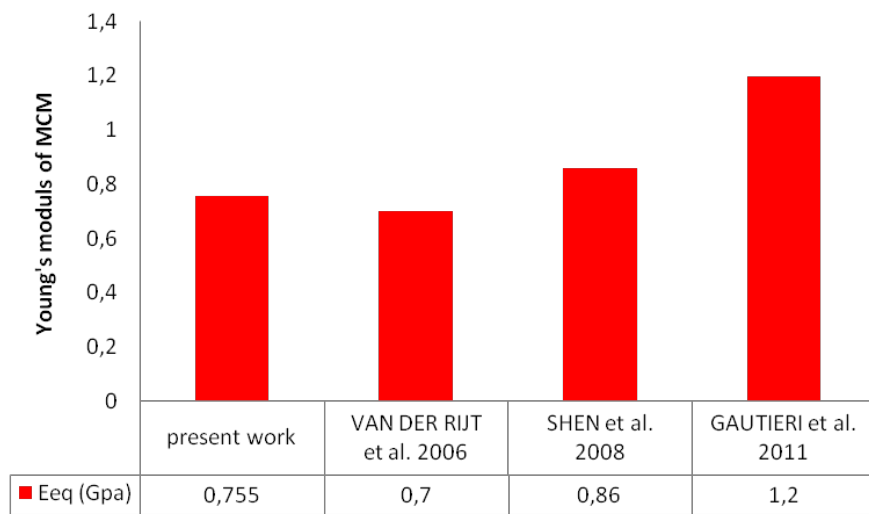


Figure 8

